Semi-active optimization of 2D wave's dispersion into mechanical systems by the mean of periodically distributed shunted piezoelectric patches: a new class of adaptive metamaterials

M. Collet[a], M. Ouisse[a], M. Ichchou[b] and M. Ruzzene[c]

[a]Dept Applied Mechanics, FEMTO-ST UMR 6174, 24 chemin de l'Epitaphe, 25 000 Besanon, France;
[b]LTDS, CNRS UMR5513, Ecole Centrale de Lyon, 36 av Guy de Collongue, 69134 Ecully, France;
[c]Georgia Institute of Technology, Aerospace School of Engineering, Atlanta, GA 30332-0405, USA.

ABSTRACT

In this paper, we present an application of the Floquet-Bloch theorem in the context of electrodynamics for vibroacoustique power flow optimization by mean of distributed and shunted piezoelectric patches. The main purpose of this work is first to propose a dedicated numerical approach able to compute the multi-modal wave dispersions curves into the whole first Brillouin zone for periodically distributed 2D shunted piezo-mechanical systems. By using a specific indicator evaluating the evanescent part Bloch's waves, we optimize, in a second time, the piezoelectric shunting electrical impedance for controlling energy diffusion into the proposed semi-active distributed set of cells. A 3D modeling of semi-distributed distribution of the optimal smart metamaterial is used for validating the obtained cell design.

Keywords: Distributed control, 2D Waves Dispersion, Bloch Theorem, Shunted piezoelectric, Mid-Frequency Optimization

1. INTRODUCTION

Tailoring the dynamical behavior of wave-guide structures can provide an efficient and physically elegant approach for optimizing mechanical components with regards to vibration and acoustic criteria, among others. However, achieving this objective may lead to different outcomes depending on the context of the optimization. In the preliminary stages of a product's development, one mainly needs optimization tools capable of rapidly providing global design directions. Such optimization will also depend on the frequency range of interest. One usually discriminates between the low frequency (LF) range and the medium frequency (MF) range, especially if vibration and noise are considered. However, it should be noted that LF optimization of vibration is more common in the literature than MF optimization. For example, piezoelectric materials and other adaptive and smart systems are employed to improve the vibroacoustic quality of structural components, especially in the LF range[1–3] even if ditributed transducers are used.[4,5] Recently, much effort has been spent on developing new multi-functional structures integrating electro-mechanical systems in order to optimize their vibroacoustic behavior over a larger frequency band of interest.[6–14] However, there is still a lack of studies in the literature for MF optimization of structural vibration. To that end, the focus of this study is to provide a suitable numerical tool for computing wave dispersion in 2D periodic systems incorporating controlling electronics devices. The main final aim is to allow their optimization in order to optimize vibroacoustic diffusion in 2D wave guides.
Two numerical approaches can be distinguished for computing that dispersion: the semi-analytical finite element method (SAFE) and the wave finite element (WFE) method. The main disadvantage of the SAFE method is that

Further author information: (Send correspondence to M. Collet)
M. Collet: E-mail: manuel.collet@univ-fcomte.fr, Telephone: 3 381 666 728

FE used are not standard so they must be specifically defined for each application. Nevertheless, a large amount of FE has been developed since 1975 to compute dispersion curves of rails,[15] laminated composite plates[16,17] and viscoelastic laminated composite plates.[18] To avoid development of specific FE, the WFE method considers the structures as periodic in order to model, with standard FE, a period of the structure. By using the periodic structure theory (PST) introduced by Mead,[15] an eigenvalue problem can be formulated from the stiffness and mass matrices of the FE model to find wave numbers of all the propagating waves. Contrary to SAFE method, the displacement field is now approximated in the direction of propagation. Thus, some numerical issues can arise when the size of FE are too coarse. As recommended by Mace and Manconi,[16] a minimum of six elements per wavelength is a good rule of thumb to ensure a reliable analysis. The WFE method has been successfully used to deal with wave propagation in two dimensional structures.[19,20] One of the main problem all these approaches is the difficulty to compute the damped wave numbers in the whole Brillouin domain necessary for optimizing vibroacoustic behavior of smart periodic structures.
After recalling the Floquet-Bloch theorems, we introduce a new numerical formulation for computing the multi-modal damped wave numbers dispersion in the whole first Brillouin domain of a periodical smart structure made of periodically distributed shunted piezoelectric patches. Based on this wave modeling, optimization of the electrical impedance of the shunted circuit is made in order to decrease group velocity of flexural waves. The obtained optimal impedance is also tested in controlling the HF response of a semi-distributed system.

2. PIEZO-ELASTO-DYNAMICAL APPLICATION OF THE FLOQUET-BLOCH THEOREM

In this section the application of the celebrated Floquet-Bloch theorem is presented for piezo-elastodynamic problems. Based on the well known results obtained by Floquet[21] in one-dimensional and later rediscovered by Bloch[22] in multidimensional problems, we propose an original application to bi-dimensional piezo-elastodynamical problem leading to very general numerical implementation for computing waves dispersion for periodically smart distributed mechanical systems incorporating electronic components and damping effects.[23]

2.1 The Bloch Theorem

The Bloch theorem gives the form of homogeneous states of Schrödinger equation with periodic potential. This theorem can be considered as a multidimensionnal application of the Floquet theorem.[24] The periodic medium (or potential) properties satisfy $M(\boldsymbol{x}+R.\boldsymbol{m})=M(\boldsymbol{x})$, $\boldsymbol{m}\in\mathbb{Z}^3$ where $R=[\boldsymbol{r}_1,\boldsymbol{r}_2,\boldsymbol{r}_3]\in\mathbb{R}^{3\times3}$ is a matrix grouping the three lattice's basis vectors (in 3D). We can also define the primitive cell as a convex polyhedron of $\mathbb{R}^3$ called Ω_x. The reciprocal unit cell is denoted by Ω_k limited by the reciprocal lattice vector defined by the three vectors $\boldsymbol{g}_j$ so that: $\boldsymbol{r}_i.\boldsymbol{g}_j=2\pi\delta_{ij}$ ($\delta_{i,j}$ the Kronecker index). We note $G=[\boldsymbol{g}_1,\boldsymbol{g}_2,\boldsymbol{g}_3]$ the reciprocal lattice matrix in the later. If Ω_x is the irreductible primitive cell, Ω_k corresponds to the first Brillouin zone of the lattice. One can see[25] for details.

The Bloch Theorem stipulates that any functions $\boldsymbol{u}(\boldsymbol{x})\in L^2(\mathbb{R}^3,\mathbb{C}^n)$ can be expressed as

$$\boldsymbol{u}(\boldsymbol{x})=\int_{\Omega_k}e^{i\boldsymbol{k}\boldsymbol{x}}\tilde{\boldsymbol{u}}(\boldsymbol{x},\boldsymbol{k})d\boldsymbol{k} \tag{1}$$

where the Bloch amplitude $\tilde{\boldsymbol{u}}(\boldsymbol{x},\boldsymbol{k})$ is Ω_x-periodic and has the representations

$$\begin{aligned}\tilde{\boldsymbol{u}}(\boldsymbol{x},\boldsymbol{k}) &= \sum_{\boldsymbol{n}\in\mathbb{Z}^3}\hat{\boldsymbol{u}}(\boldsymbol{k}+G\boldsymbol{n})e^{iG\boldsymbol{n}.\boldsymbol{x}},\\ \boldsymbol{u}(\boldsymbol{x}) &= \frac{|\Omega_x|}{(2\pi)^3}\sum_{\boldsymbol{n}\in\mathbb{Z}^3}\boldsymbol{u}(\boldsymbol{x}+R\boldsymbol{n})e^{i\boldsymbol{k}(\boldsymbol{x}+R\boldsymbol{n})}\end{aligned} \tag{2}$$

where $\hat{\boldsymbol{u}}(\boldsymbol{k})$ stands for the Fourier transform of $\boldsymbol{u}(\boldsymbol{x})$. One can also demonstrate that the mean value of the Bloch amplitude is the Fourier amplitude of $\boldsymbol{u}(\boldsymbol{x})$ for the corresponding wave vector: $\langle\tilde{\boldsymbol{u}}(.,\boldsymbol{k})\rangle_{\Omega_x}=\hat{\boldsymbol{u}}(\boldsymbol{k})$. Using the Bloch theorem to represent the solutions of periodical partial derivative equations implies that all derivatives are shifted by $\boldsymbol{k}$ in the sense given by the used spatial operator.

Based on that theorem one can define the expansion functions $\boldsymbol{v}_m(\boldsymbol{x},\boldsymbol{k})$, called the Bloch eigen modes, such that they can be used to represent the Bloch amplitudes of any solution of the corresponding partial derivative equation as

$$\tilde{\boldsymbol{u}}(\boldsymbol{x},\boldsymbol{k}) = \sum_m \boldsymbol{u}_m(\boldsymbol{k})\boldsymbol{v}_m(\boldsymbol{x},\boldsymbol{k}) \tag{3}$$

and at the same time diagonalize the partial derivative equations. One notes that the expansion coefficients $\boldsymbol{u}_m(\boldsymbol{k})$ depend on the applied disturbance and also on the induced wave vector (see[26] for details).

2.2 Application to Piezo-Elastodynamic

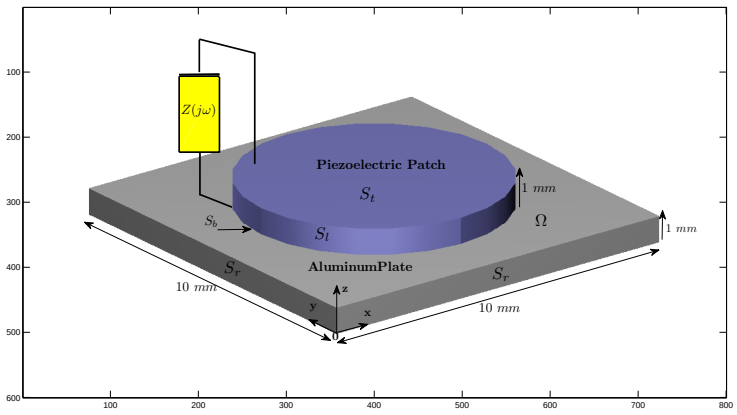

Figure 1. Generic 3D piezocomposite periodic cell

Let us consider a piezo-elastodynamic problem made of infinite periodic distribution of unitary cell described in figure 1. The harmonic homogeneous dynamical equilibrium of system is driven by the following partial derivative equation :

$$\begin{cases} \rho\ddot{\boldsymbol{w}}(\boldsymbol{x}) - \nabla\sigma(\boldsymbol{x}) = 0 & \forall \boldsymbol{x} \in \Omega_x \\ -\nabla D(\boldsymbol{x}) = 0 & \forall x \in \Omega_x \end{cases} \tag{4}$$

where $\boldsymbol{w}(\boldsymbol{x}) \in \mathbb{R}^3(\Omega_x)$ is the displacement vector, σ represents the Cauchy stress tensor, $\epsilon = \nabla_{sym} w = \frac{1}{2}(\nabla w^T(x) + w(x)\nabla^T)$ the Green strain tensor, $D(\boldsymbol{x})$ the electric displacement. The linear constitutive material behavior relationships can be written as

$$\sigma = C_E(\boldsymbol{x})\epsilon - e^T(\boldsymbol{x})\boldsymbol{E} \tag{5}$$

$$\boldsymbol{D} = e(\boldsymbol{x})\epsilon + \varepsilon_S(\boldsymbol{x})\boldsymbol{E} \tag{6}$$

where $\boldsymbol{E} = -\nabla V$ the electric field vector (V the voltage), C_E the elasticity tensor at constant electrical field, e^T the piezoelectric coupling tensor and ε_S the dielectric permittivity at constant strain. We add to this set of equilibrium equations an output expression

$$q^o = -\int_{S_t} \boldsymbol{D}.\boldsymbol{n} dS \tag{7}$$

allowing the introduction of the charge measurement on the piezoelectric's top electrode and hence the dual counterpart of the imposed electrical Dirichlet boundary condition for applying the shunt impedance operator. The equations above are consistent for each kind of material to the extent that null piezoelectric and permittivity tensors can be used when passive materials are considered. All of these tensors also depend on the spatial location vector $\boldsymbol{x}$. The piezo-elastodynamic equilibrium can also be written as :

$$\rho\omega^2\boldsymbol{w}(\boldsymbol{x}) + \nabla C\nabla_{sym}(\boldsymbol{w}(\boldsymbol{x})) + \nabla e^T(\boldsymbol{x})\nabla V(\boldsymbol{x}) = 0 \ \forall \boldsymbol{x} \in \Omega_x \tag{8}$$

$$-\nabla e(x)\nabla_{sym}(\boldsymbol{w}(\boldsymbol{x})) + \nabla\varepsilon_S(x)\nabla V(\boldsymbol{x}) = 0 \ \forall \boldsymbol{x} \in \Omega \tag{9}$$

As the problem is 2D infinitely periodic, only electrostatic boundary conditions have to be considered on each cell:

$$\begin{cases} V = 0 & \forall x \in S_b \\ V = V^o & \forall x \in S_t \\ \boldsymbol{D}.\boldsymbol{n} = 0 & \forall x \in S_l \end{cases} \tag{10}$$

where S_b is the grounded bottom electrode of the piezoelectric layer, S_t is the top electrode connected to the external shunt and s_l the lateral electrode less boundary. The top electrode applied feedback voltage V_o depends on the shunt characteristic and on the collected charges q^o (7) and can be expressed in the Fourier space by:

$$V^o(i\omega) = -Z(i\omega)q^o(i\omega) \tag{11}$$

By considering a primitive cell of the periodic problem Ω_x and by using the Bloch theorem, we can compute the associated Bloch eigenmodes (3) and the dispersion functions by searching the eigen solutions of the homogeneous problem (8) and (9) as:

$$\boldsymbol{u}(\boldsymbol{x}) = \begin{bmatrix} \boldsymbol{w}(\boldsymbol{x}) \\ V(\boldsymbol{x}) \end{bmatrix} = \boldsymbol{u}_{n,k}(\boldsymbol{x}) e^{i\boldsymbol{k}.\boldsymbol{x}} \tag{12}$$

with $\boldsymbol{u}_{n,\boldsymbol{k}}(\boldsymbol{x}) = \begin{bmatrix} \boldsymbol{w}_{n,\boldsymbol{k}}(\boldsymbol{x}) \\ V_{n,\boldsymbol{k}}(\boldsymbol{x}) \end{bmatrix}$, Ω_x periodic functions. By introducing expression (12) in the piezo-elastidynamic equations (8), (9), one can demonstrate that $\boldsymbol{w}_{n,\boldsymbol{k}}(\boldsymbol{x})$, $V_{n,\boldsymbol{k}}(\boldsymbol{x})$ and $\omega_n(\boldsymbol{k})$ are solutions of the generalized eigenvalues problem:

$$\begin{aligned} &\rho\omega_n^2(\boldsymbol{k})\boldsymbol{w}_{n,\boldsymbol{k}}(\boldsymbol{x}) + \nabla C\nabla_{sym}(\boldsymbol{w}_{n,\boldsymbol{k}}(\boldsymbol{x})) + ik\left\{(C\nabla_{sym}(\boldsymbol{w}_{n,\boldsymbol{k}}(\boldsymbol{x}))).\boldsymbol{\Phi} + \nabla(C\Xi_{n,\boldsymbol{k}}(\boldsymbol{x}))\right\} - k^2(C\Xi_{n,k}(\boldsymbol{x})).\boldsymbol{\Phi} \\ &\quad +\nabla e^T\nabla V_{n,\boldsymbol{k}}(\boldsymbol{x}) + ik\left\{(\nabla e^T V_{n,\boldsymbol{k}}(\boldsymbol{x})).\boldsymbol{\Phi} + (e^T\nabla V_{n,\boldsymbol{k}}(\boldsymbol{x})).\boldsymbol{\Phi}\right\} - k^2 V_{n,\boldsymbol{k}}(\boldsymbol{x})(e^T\boldsymbol{\Phi}).\boldsymbol{\Phi} = 0 \quad \forall \boldsymbol{x} \in \Omega_x \end{aligned} \tag{13}$$

$$\begin{aligned} &-\nabla e\nabla_{sym}(\boldsymbol{w}_{n,\boldsymbol{k}}(\boldsymbol{x})) - ik\left\{\nabla(e\Xi_{n,\boldsymbol{k}}(\boldsymbol{x})) + (e\nabla_{sym}(\boldsymbol{w}_{n,\boldsymbol{k}}(\boldsymbol{x})))\right\}.\boldsymbol{\Phi}\} + k^2(e\Xi_{n,\boldsymbol{k}}(\boldsymbol{x})).\boldsymbol{\Phi} \\ &\quad +\nabla\varepsilon_S\nabla V_{n,\boldsymbol{k}}(\boldsymbol{x}) + ik\left\{(\nabla\varepsilon_S V_{n,\boldsymbol{k}}(\boldsymbol{x})).\boldsymbol{\Phi} + (\varepsilon_S\nabla V_{n,\boldsymbol{k}})(\boldsymbol{x}).\boldsymbol{\Phi}\right\} - k^2(\varepsilon_S\boldsymbol{\Phi}V_{n,\boldsymbol{k}}(\boldsymbol{x})).\boldsymbol{\Phi} = 0 \quad \forall \boldsymbol{x} \in \Omega_x \end{aligned} \tag{14}$$

with the associated bounadry conditions :

$$\begin{cases} \boldsymbol{w}_{n,\boldsymbol{k}}(\boldsymbol{x} - R.\boldsymbol{m}) = \boldsymbol{w}_{n,\boldsymbol{k}}(\boldsymbol{x}) & \forall \boldsymbol{x} \in S_r \ \boldsymbol{m} \in \mathbb{Z}^2 \\ V_{n,\boldsymbol{k}}(\boldsymbol{x}) = 0 & \forall \boldsymbol{x} \in S_b \\ V_{n,\boldsymbol{k}}(\boldsymbol{x})V = -Z(i\omega)q^o_{n,\boldsymbol{k}} & \forall \boldsymbol{x} \in S_t \\ \boldsymbol{D}.\boldsymbol{n} = 0 & \forall \boldsymbol{x} \in S_l \end{cases}$$

where $\boldsymbol{k} = k\begin{bmatrix} cos(\phi) \\ sin(\phi) \\ 0 \end{bmatrix} = k\boldsymbol{\Phi}$ where ϕ represent the direction angles into the reciprocal 2D lattice domain and $\Xi_{n,\boldsymbol{k}}(\boldsymbol{x}) = \frac{1}{2}(\boldsymbol{w}_{n,\boldsymbol{k}}(\boldsymbol{x}).\Phi^T + \Phi.\boldsymbol{w}^T_{n,\boldsymbol{k}}(\boldsymbol{x}))$ the symmetric dyadic tensor or the dyadic product of the displacement $\boldsymbol{w}_{n,\boldsymbol{k}}(\boldsymbol{x})$ and direction vector Φ. S_r are the interface of the cells continuum, and R the matrix grouping the two lattice's basis vectors (in 2D in the considered problem). In the electrical boundary conditions, $q^t_{n,\boldsymbol{k}}$ is given by :

$$q^o_{n,\boldsymbol{k}} = \int_{S_t} [-e(\nabla_{sym}(\boldsymbol{w}_{n,\boldsymbol{k}}(\boldsymbol{x})) + ik\nabla e\Xi_{n,\boldsymbol{k}}(\boldsymbol{x})) + \varepsilon_S(\nabla V_{n,\boldsymbol{k}}(\boldsymbol{x}) + ikV_{n,\boldsymbol{k}}(\boldsymbol{x})\boldsymbol{\Phi}].\boldsymbol{n}dS \tag{15}$$

where $\boldsymbol{n}$ is the outpointing unitary normal vector.
The proposed formulation is also based on the computation of the Floquet vectors (equation (13), (14)), instead of computing the Floquet propagators commonly used for elastodynamic applications. Our approach allows to obtain the full 2D waves dispersions functions and to clearly introduce damping and electrical impedance into the piezo-elastodynamic operator. The adopted methodology allows the computation of the complete complex map of the dispersion curves incorporating computation of evanescent waves and allowing the introduction of damping and shunt operator if any.

2.3 Weak Formulation and computation of waves dispersion functions in periodical piezo-composite lattice

Let us consider the partial derivative equations (13), (14) on a unit cell Ω. It stands for a generalized eigenvalue problem leading to compute the dispersion functions $\omega_n(\boldsymbol{k})$ and the corresponding Floquet eigenvectors $\boldsymbol{u}_{n,\boldsymbol{k}}(\boldsymbol{x})$. For computing the 2D dispersions curves, we need to introduce a suitable weak formulation.
If $\boldsymbol{u}_{n,\boldsymbol{k}}(\boldsymbol{x})$ is a solution of equations (13), (14), also $\forall \tilde{\boldsymbol{w}}_{n,\boldsymbol{k}}(\boldsymbol{x}) \in \left\{H_1(\Omega,\mathbb{C}^3)/\tilde{\boldsymbol{w}}_{n,\boldsymbol{k}}(\boldsymbol{x}-R\boldsymbol{m}) = \tilde{\boldsymbol{w}}_{n,\boldsymbol{k}}(\boldsymbol{x})\ \forall \boldsymbol{x} \in S_r\right\}$ and $\tilde{V}_{n,\boldsymbol{k}}(\boldsymbol{x}) \in \left\{H_1(\Omega,\mathbb{C})/\tilde{V}_{n,k}(\boldsymbol{x}) = 0\ \forall \boldsymbol{x} \in S_b \text{ and } \tilde{V}_{n,k}(\boldsymbol{x}) = V^o\ \forall \boldsymbol{x} \in S_t\right\}$ we have :

$$\int_\Omega \rho\omega_n^2(\boldsymbol{k})\tilde{\boldsymbol{w}}_{n,\boldsymbol{k}}(\boldsymbol{x})w_{n,\boldsymbol{k}}(\boldsymbol{x}) - (\tilde{\varepsilon}_{n,\boldsymbol{k}}(\boldsymbol{x}) - ik\tilde{\Xi}_{n,\boldsymbol{k}}(\boldsymbol{x}))C(\varepsilon_{n,\boldsymbol{k}}(\boldsymbol{x}) + ik\Xi_{n,\boldsymbol{k}}(\boldsymbol{x}))$$
$$+(\tilde{\varepsilon}_{n,\boldsymbol{k}}(\boldsymbol{x}) - ik\tilde{\Xi}_{n,\boldsymbol{k}}(\boldsymbol{x}))e^T(\nabla V_{n,\boldsymbol{k}}(\boldsymbol{x}) + ikV_{n,\boldsymbol{k}}(\boldsymbol{x})\boldsymbol{\Phi}) - (\nabla\tilde{V}_{n,\boldsymbol{k}}(\boldsymbol{x}) - ik\tilde{V}_{n,\boldsymbol{k}}(\boldsymbol{x})\boldsymbol{\Phi})e(\varepsilon_{n,\boldsymbol{k}}(\boldsymbol{x}) + ik\Xi_{n,\boldsymbol{k}}(\boldsymbol{x}))$$
$$+(\nabla\tilde{V}_{n,\boldsymbol{k}}(\boldsymbol{x}) - ik\tilde{V}_{n,\boldsymbol{k}}(\boldsymbol{x})\boldsymbol{\Phi})\varepsilon_S(\nabla V_{n,\boldsymbol{k}}(\boldsymbol{x}) + ikV_{n,\boldsymbol{k}}(\boldsymbol{x})\boldsymbol{\Phi})d\Omega - \frac{\tilde{V}^t_{n,\boldsymbol{k}}V^t_{n,\boldsymbol{k}}}{Z(i\omega)} \quad = 0 \tag{16}$$

This weak formulation is simply obtained by integrating equation (13), (14) projected onto any test function $\tilde{u}_{n,\boldsymbol{k}}(\boldsymbol{x})$. The boundary integral vanishes as the test functions are chosen so that $\tilde{\boldsymbol{w}}_{n,\boldsymbol{k}}(\boldsymbol{x}-R\boldsymbol{m}) = \tilde{\boldsymbol{w}}_{n,\boldsymbol{k}}(\boldsymbol{x})$ on S_r. For a polyhedron cell, each boundary is generally a polyhedral plane sub-domain that can be associated with a parallel opposite one. The symmetry conditions called $\tilde{\boldsymbol{w}}_{n,\boldsymbol{k}}(\boldsymbol{x}-R\boldsymbol{m}) = \tilde{\boldsymbol{w}}_{n,\boldsymbol{k}}(\boldsymbol{x})$ explicitly link these associated surfaces.

2.4 Numerical Computation of the Bloch's waves

The numerical implementation is obtained by using a standard finite elements method to discretize the weak formulation (16). The assembled matrix equation is given by:

$$(K(Z(i\omega_n(\lambda,\phi)) + \lambda L(\phi, Z(i\omega_n(\lambda,\phi))) - \lambda^2 H(\phi, Z(i\omega_n(\lambda,\phi))) - \omega_n^2(\lambda,\phi)M)u_{n,k}(\phi) = 0, \tag{17}$$

where $\lambda = ik$, M and $K(Z(i\omega_n(\lambda,\phi)))$ are respectively the standard symmetric semi-definite mass and stiffness matrices (the mass matrix is semi definite because elastostatic equation are condensed into the equation), $L(\phi, Z(i\omega_n(\lambda,\phi)))$ is a skew-symmetric matrix and $H(\phi, Z(i\omega_n(\lambda,\phi)))$ is a symmetric semi-definite positive matrix.

When k and ϕ are fixed and Z does not depend on ω the system (17) is a linear eigen value problem allowing us to compute the dispersion functions $\omega_n^2(\boldsymbol{k},\phi)$ and the associated Bloch eigenvector $\boldsymbol{u}_{n,k}(\phi)$.

This approach has been widely used for developing homogenization techniques and spectral asymptotic analysis like in the work of.[27] It can also be applied for computing wave's dispersion even if Floquet propagators is preferred for 1D or quasi 1D computation, as indicated in.[28–30] Nevertheless these approaches have been only developed for undamped mechanical systems that is to say represented by a set of real matrices. In this case, most of the previously published works present techniques based on the mesh of a real $\boldsymbol{k}$-space (i.e $\boldsymbol{k}$ or λ and ϕ) inside the first Brillouin zone for obtaining the corresponding frequency dispersion and the associated Floquet vectors. For undamped system only propagative or evanescent waves exist corresponding to a family of eigen solutions purely real or imaginary. Discrimination between each class of waves is easy. If a damped system is considered (K, L, H are complex frequency dependent) or frequency dependence of the electrical shunt impedance is considered, the obtained eigenvalue problem is not quadratic and a complex specific numerical methodology has to be implemented. Furthermore, evanescent part of propagating waves appear as the imaginary part of $\omega_n^2(\lambda,\Phi)$. It then becomes very difficult to distinguish the propagative and evanescent waves but also to compute the corresponding physical wave's movements by applying spatial deconvolution.

Another much more suitable possibility for computing damped system, dedicated for time/space deconvolution and for computation of diffusion properties as defined by,[6,30] is to consider the following generalized eigen value problem:

$$(K(Z(\omega) - \omega^2 M + \lambda_n(\omega,\phi)L(\phi,Z(\omega)) - \lambda_n^2(\omega,\phi)H(\phi,Z(\omega)))u_n(\omega,\phi) = 0. \tag{18}$$

In this problem, the pulsation ω is a real parameter corresponding to the harmonic frequency. Wave's numbers and Floquet vectors are then computed. An inverse Fourier transformation in the k-space domain can lead us to evaluate the physical wave's displacements and energy diffusion operator when the periodic distribution is connected to another system as in.[6] Another temporal inverse Fourier transformation can furnish a way to access spatio-temporal response for non-homogeneous initial conditions. As L is skew-symmetric, the obtained eigen values are quadruple $(\lambda, \bar{\lambda}, -\lambda, -\bar{\lambda})$ collapsing into real or imaginary pairs (or a single zero) when all matrices are real (i.e. for an undamped system). In this case a real pair of eigen values correspond to evanescent modes oriented in two opposite directions on the k-space and imaginary values to two traveling waves propagating in opposite direction.

As previously mentioned, the real part of $\boldsymbol{k} = k\boldsymbol{\Phi}$ vector is restricted to stand inside the first Brillouin zone. In the quadratic eigen value problem (18) nothing restricts computation to only find eigen values satisfying this condition. For direction vector $\boldsymbol{\Phi}$ orthogonal to the lattice facelets (i.e. for $\Phi_{p1} = [1, 0]^T$ and $\Phi_{p2} = [0, 1]^T$ in bi-dimensional rectangular cell), the periodical conditions expressed for one dimensional wave guide are still valid: if $\lambda_j(\omega, \boldsymbol{\Phi}_p)$ is an eigen value associated to $\boldsymbol{w}_j(\omega, \boldsymbol{\Phi}_p)$ then $\forall \boldsymbol{m} \in \mathbb{Z}^3$, $\lambda + i.\boldsymbol{\Phi}_p^T(G.\boldsymbol{m})$ is also an eigen value associated to $\boldsymbol{w}_j(\omega, \boldsymbol{\Phi}_p)e^{-i.\boldsymbol{\Phi}_p^T(G.\boldsymbol{m})x}$. Thus, for undamped systems, all obtained eigenvalues are periodically distributed in the $\boldsymbol{k}$-space along its principal directions.

2.5 Computation of the group velocity and evanescence criterion

The main aim of this paper is to provide a numerical methodology for optimizing the piezoelectric shunt impedance $Z(\omega)$ for controlling energy flow into the periodically distributed piezo-composite structure. For doing this, we need to define a suitable criterion. The waves group velocities indicate how energy is transported into the considered system and allow to distinguish the 'propagative' and 'evanescent' waves. If one Bloch eigen solution (i.e $u_n(\omega, \phi),\ k_n(\omega)$) is considered, the associated group velocity vector[31] is given by :

$$\boldsymbol{C}_{g_n}(\omega, \phi) = \nabla_{\boldsymbol{k}}\omega = \frac{\langle\langle \boldsymbol{S} \rangle\rangle}{\langle\langle e_{tot} \rangle\rangle} = \frac{\langle \boldsymbol{I} \rangle}{\langle E_{tot} \rangle} \tag{19}$$

where $\langle\langle : \rangle\rangle$ is the spatial and time average respectivelly on one cell and one period, $\boldsymbol{S}$ is the density of energy flux defined in,[31] $\boldsymbol{I}$ the mean intensity and e_{tot}, E_{tot} the total piezomechanical energy and its time average on a period (see[31] for details). In this problem, we only consider mechanical energy transportation as the electrostatic coupling is decentralized and can be condensed as a mechanical interface as proved in[32] and generally computed in.[33] So we also compute the intensity vector $\boldsymbol{I}$ by :

$$\langle \boldsymbol{I}_n \rangle = -\frac{\omega}{2} Re\Big(\int_{\Omega_x} C(\varepsilon_n(\boldsymbol{x}, \omega, \phi) + ik\Xi_n(\boldsymbol{x}, \omega, \phi)).(\boldsymbol{w}_n^*(\boldsymbol{x}, \omega, \phi))d\Omega/V_{ol} \tag{20}$$

where $.^*$ is the complex conjugate and V_{ol} the domain volume. As the spatio-temporal average of the system Lagragian is null (see[31]), the total energy average is approximated by only computing the kinetic energy average:

$$\langle E_{tot} \rangle = \frac{1}{2}\Big(\int_{\Omega_x} \rho\omega^2 \boldsymbol{w}_n(\boldsymbol{x}, \omega, \phi).\boldsymbol{w}_n^*(\boldsymbol{x}, \omega, \phi)d\Omega/V_{ol} \tag{21}$$

The group velocity vectors $\boldsymbol{C}_{g_n}(\omega, \phi)$ is computed for all wave numbers at each frequency. In order to focus our analysis on only flexural modes (S and SH ones) we introduce an indicator allowing to select them by computing the ratio of kinetic energy average on out of plane displacement as:

$$Ind(n, \omega, \phi) = \frac{\frac{1}{2}(\int_{\Omega_x} \rho\omega^2 wz_n(\boldsymbol{x}, \omega, \phi) wz_n^*(\boldsymbol{x}, \omega, \phi)d\Omega/V_{ol}}{\langle E_{tot} \rangle} \tag{22}$$

with $wz_n(\boldsymbol{x}, \omega, \phi)$ being the (Oz) component of vector $\boldsymbol{w}_n(\boldsymbol{x}, \omega, \phi)$.

Piezoelectric Material		
Symbol	Value	Property
$s_{11}^E = s_{22}^E = s33^E$	$11.6 \times 10^{-12}\ Pa^{-1}$	11, 22 and 33 compliance matrix coefficients
$s_{12}^E = s_{13}^E = s_{23}^E$	$-3.33 \times 10^{-12}\ Pa^{-1}$	12, 13 and 23 compliance matrix coefficient
$s_{44}^E = s_{55}^E = s_{66}^E$	$45.0 \times 10^{-11}\ Pa^{-1}$	44, 55 and 66 compliance matrix coefficients
η	0.1 %	Hysteretic Damping ratio
$d_{31} = d_{32}$	$-6 \times 10^{-11}\ C/N$	31 and 32 piezoelectric matrix coefficients
d_{33}	$15.2 \times 10^{-11}\ C/N$	33 piezoelectric matrix coefficient
$d_{24} = d_{15}$	$730 \times 10^{-12}\ C/N$	24 and 15 piezoelectric matrix coefficients
ρ	$7600 kg/m^3$	Density
$\varepsilon_{11}^T = \varepsilon_{22}^T$	$504.1\ \varepsilon_o\ C/V/m$	Dielectric Permittivity
ε_{33}^T	$270\ \varepsilon_o\ C/V/m$	Dielectric Permittivity

Table 1. *Piezoelectric patch characteristics*

3. OPTIMISATION OF THE FLEXURAL ENERGY FLOW INSIDE THE SHUNTED PERIODIC PIEZO-COMPOSITE

The considered piezo-composite cell is presented in figure 1. The supporting plate material is standard aluminum with 0.1 % of hysteretic damping ratio and the piezoelectric material characteristics is given in table 1.

The used methodology for optimizing the shunt impedance $Z(i\omega)$ is based on the minimization of the maximal group velocity collinear to the wave number vector (19) for waves having a ratio of transported flexural kinetic energy (22) greater than 0.8. The used criterion can also be written as:

$$Crit(Z(i\omega), \phi) = max_{n/Ind(n,\omega,\phi)>0.8}(\boldsymbol{C}_{g_n}(\omega, \phi).\boldsymbol{\Phi}) \tag{23}$$

The used numerical optimization of the criteria is based on a multidimensional unconstrained nonlinear minimization (Nelder-Mead).

3.1 Case 1 : $Z(i\omega) \in \mathbb{C}$

In a first test, we optimize the criterion by considering any frequency dependent complex impedance. We present in figure 2(a) and 2(b) the obtained real parts and imaginary parts of the wave number $kx_n(i\omega)$ along (Ox) axis. The red circles mark the dispersions curves for $Z = 0$ and the blue crossed the optimal dispersion. The corresponding group velocities along (Ox) are presented in figure 3 while the real and imaginary parts of the optimal impedance are plotted in figure 4.

We immediately observe that the optimization of the shunt impedance leads to greatly modify the group velocity of the A_o mode in the first part of the spectrum (i.e before the first bending band gap between 22 and 27 kHz). The bending waves also propagate energy with a lower velocity and can even been very low as evanescent waves before 6 kHz. The corresponding real and imaginary parts of the dispersion curves are slightly modified. We notice an increase of the imaginary values indicating an increase of the spatial decay rates. The optimal impedance values are almost real, and correspond to those obtained if a constant negative capacitance is used. The corresponding average value is $-150.05\ pC.V^{-1}$. Some imaginary parts of the optimal impedance are negative which indicate that the optimization leads to provide energy to the system for controlling mechanical damping effect introduced with hysteretic damping ratios into the model, and, also, obtain a fully conservative system.

3.2 Case 2 : $Z(i\omega) \in \mathbb{R}$

As the obtained negative impedance imaginary part does not appear realistic for physical implementation, the second case considers optimization by considering frequency dependent real impedance. We present in figure 5(a) and 5(b) the obtained real parts and imaginary parts of the wave number $kx_n(i\omega)$ along (Ox) axis. The red circles mark the dispersions curves for $Z = 0$ and the blue crossed the optimal dispersion. The corresponding group velocities along (Ox) is presented in figure 6 while the real and imaginary parts of the optimal impedance are plotted in figure 7.

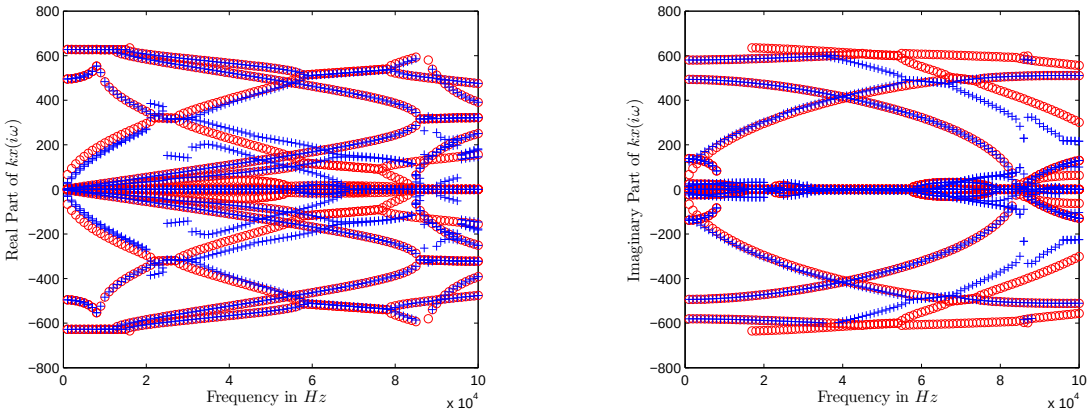

(a) a (b) b

Figure 2. Real parts (a) and imaginary parts (b) of the wave number $kx_n(i\omega)$ along (Ox), the red circles mark values obtained for $Z = 0$ and the blue crossed the optimal ones

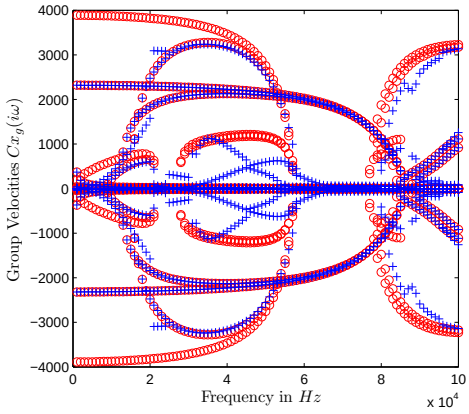

Figure 3. Group velocities along (Ox) direction; the red circles mark values obtained for $Z = 0$ and the blue crossed the optimal ones

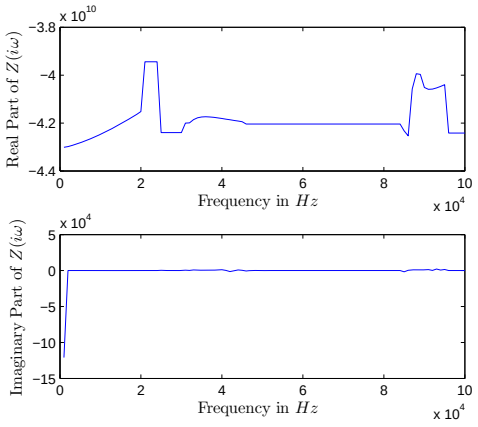

Figure 4. Real and imaginary parts of the optimal impedance

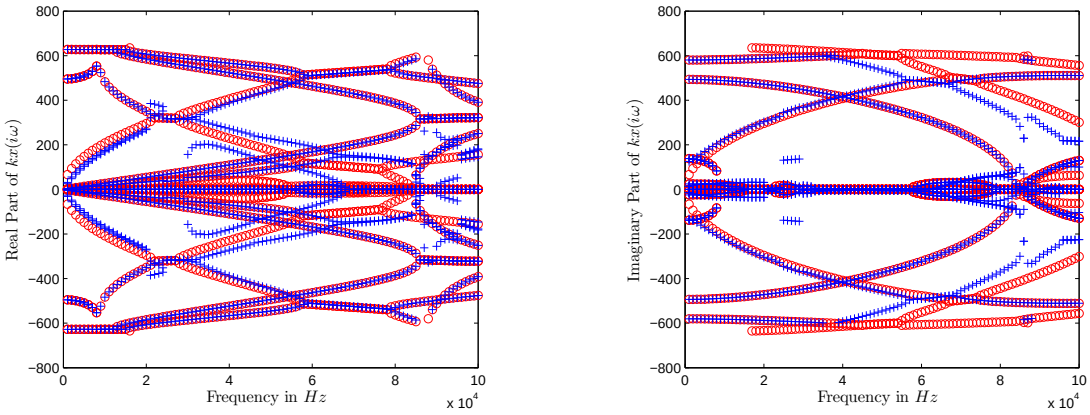

(a) a (b) b

Figure 5. Real parts (a) and imaginary parts (b) of the wave number $kx_n(i\omega)$ along (Ox), the red circles mark values obtained for $Z = 0$ and the blue crossed the optimal ones

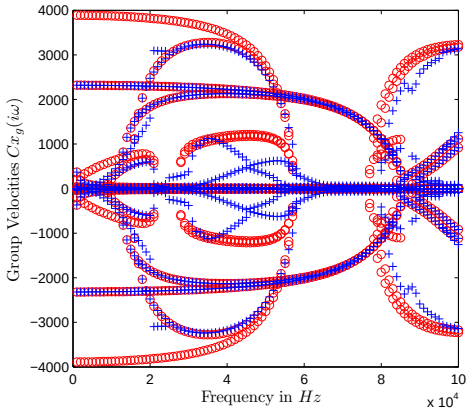

Figure 6. Group velocities along (Ox) direction; the red circles mark values obtained for $Z = 0$ and the blue crossed the optimal ones

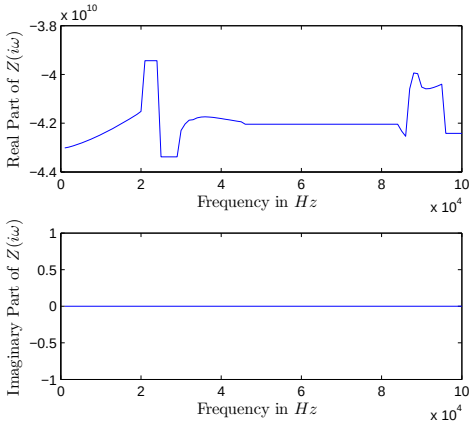

Figure 7. Real and imaginary parts of the optimal impedance

We immediately observe that the obtained results are globally similar to those provided by the complete complex optimization presented before, even if the equivalent constant negative capacitance is now -149.88 $pC.V^{-1}$. The numerical cost is lower and the optimization faster.

3.3 Validation on a periodically semi-distributed set of adaptive cells

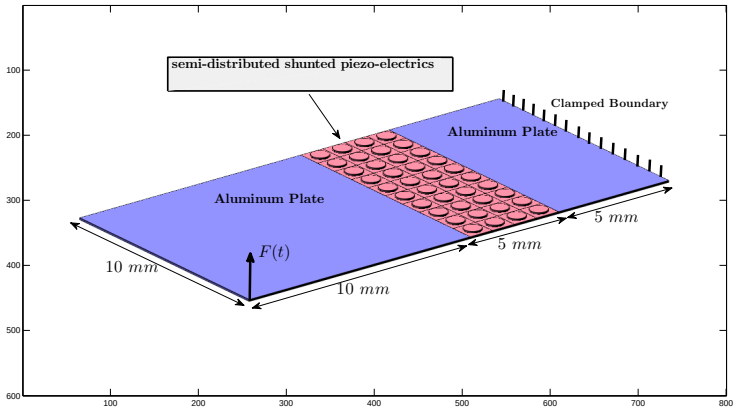

Figure 8. 3D piezocomposite periodic semi-distributed Cells

In order to study the translation of the wave properties obtained by optimizing the previously described criterion on the dynamical response of a finite dimension system, we apply the optimal impedance on a finite set of shunted piezo-composite cells semi-distributed onto a plate system as described in figure 8. The harmonic response of this system is also computed at different frequency when optimal impedance is connected or not to each patches. We plot in figure 9 the obtained results in term of kinetic energy density.

These numerical results clearly show up a strong influence of the modifications of the wave dispersion (i.e on the group velocities) in the standing wave responses plotted in figure 9. We observe at 5 kHz an increase in the dynamic response of the system when optimal shunt is connected. A large part of the system energy remains in its left part where the applied forces is located. The semi-distributed interface also change the system admittance and filter wave diffusion by increasing is reflexibility property. At 22 kHz, the energy diffusion is clearly condensed into the left part of the system with a largely decreased amplitude compared to this obtained with open circuit. The structural dynamical admittance has been decreased by connecting the shunt circuits. Finally, at 60 kHz, the energy is concentrated on the right part of the system between the adaptive interface and the clamped boundary condition. We observe something similar to a wave trap effect. The average value is, one more time, largely decrease by using the shunt circuits.

4. CONCLUSIONS

This paper presents a numerical procedure able to compute the damped wave's dispersion functions in the whole first Brillouin domain of multi dimensionnal piezo-elastodynamical wave guides. The method was applied for determining the optimal impedance allowing to minimize the group velocities of the flexural waves. Based on this approach, some numerical test on a finite dimension system incorporating a semi-distributed set of shunted piezo-composite cells has been performed. We underline a strong influence of the designed shunt circuits in the dynamical response of the system. Even if the link between the obtained wave properties are not clearly established, we also demonstrated that our developed numerical procedures can be used for optimizing the energy diffusion operator of such adaptive mechanical interface. To do so, additional work has to be done for optimizing the complete interface scattering and for controlling the evanescent waves playing an important role in the finite system dynamical response.
The proposed methodology can also be used for studying particular dissipation phenomenon such as those induced

by complex shunted piezoelectric patches as proposed by[8] and,[34] or even foams or complex polymers behaviors. The proposed method furnishes an efficient tool for future optimization of distributed smart cells as proposed in the case of 1D wave guide by.[6]

ACKNOWLEDGMENTS

This work was carried out with a grant of French agency ANR number $NT09-617542$. We gratefully acknowledge the French ANR and CNRS for supporting this program.

REFERENCES

[1] A. Preumont, *Vibration control of structures : An introduction*, Kluwer, 1997.

[2] S. P.A. Nelson, *Active Control of Sound*, Pub. Academic Press, London, San Diego, 1992.

[3] H. Banks and Y. W. R.C. Smith, *Smart material structures Modeling Estimation and Control*, Masson and Wiley, 1996.

[4] R. Batra, F. dell'Isola, S. Vidoli, and D. Vigilante, "Multimode vibration suppression with passive two-terminal distributed network incorporating piezoceramic transducers," *International Journal of Solids and Structures* **42**(11-12), pp. 3115 – 3132, 2005.

[5] H. Tzou and H. Fu, "A study of segmentation of distributed piezoelectric sensors and actuators, part i: Theorical analysis.," *Journal of Sound and Vibration* **172(2)**, pp. 247–259, 1994.

[6] M. Collet, K. Cunefare, and N. Ichchou, "Wave Motion Optimization in Periodically Distributed Shunted Piezocomposite Beam Structures," *Journal of Int Mat Syst and Struct* **20**(7), pp. 787–808, 2009.

[7] O. Thorp, M. Ruzzene, and A. Baz, "Attenuation and localization of wave propagation in rods with periodic shunted piezoelectric patches," *Proceedings of SPIE - The International Society for Optical Engineering Smart Structures and Materials* **4331**, pp. 218–238, 2001.

[8] B. Beck, K. Cunefare, and M. Ruzzene, "Broadband vibration suppression assessment of negative impedance shunts," in *Proceedings of SMASIS08*, **6928**, ASME, 2008.

[9] B. Beck, K. A. Cunefare, M. Ruzzene, and M. Collet, "Experimental analysis of a cantilever beam with a shunted piezoelectric periodic array," in *ASME-SMASIS*, ASME, (Philadelphia), Sept 28 Oct 1 2010.

[10] I. Bartoli, A. Marzani, F. L. di Scalea, and E. Viola, "Modeling wave propagation in damped waveguides of arbitrary cross-section," *Journal of Sound and Vibration* **295**, pp. 685–707, AUG 22 2006.

[11] M. Foda, A. Almajed, and M. ElMadany, "Vibration suppression of composite laminated beams using distributed piezoelectric patches," *Smart Materials and Structures* **19**(11), p. 115018, 2010.

[12] M. S. I. S. Dawood, L. Iannucci, and E. S. Greenhalgh, "Three-dimensional static shape control analysis of composite plates using distributed piezoelectric actuators," *Smart Materials and Structures* **17**(2), p. 025002, 2008.

[13] J. Jiang and D. Li, "Decentralized robust vibration control of smart structures with parameter uncertainties," *Journal of Intelligent Material Systems and Structures* , 2010.

[14] B. Y. Ren, L. Wang, H. S. Tzou, and H. H. Yue, "Finite difference based vibration simulation analysis of a segmented distributed piezoelectric structronic plate system," *Smart Materials and Structures* **19**(8), p. 085024, 2010.

[15] D. Mead, "A general theory of harmonic wave propagation in linear periodic systems with multiple coupling," *J. Sound Vibrat.* **27**(2), pp. 429–438, 1996.

[16] B. Mace and E. Manconi, "Modelling wave propagation in two-dimensional structures using finite element analysis," *Journal of Sound and Vibrations* **318**, pp. 884–902, 2008.

[17] S. Gonella and M. Ruzzene, "Analysis of in-plane wave propagation in hexagonal and re-entrant lattices," *J. Sound Vibrat.* **312**, pp. 125–139, 2008.

[18] S. Akrout, *Comportement dynamique dterministe et large bande des structures guides.* PhD thesis, cole Centrale Lyon, 2005.

[19] E. Manconi, *The Wave Finite Element Method for 2-dimensional Structures.* PhD thesis, University of Parma, 2008.

[20] J. Berthaut, M. Collet, and M. Ichchou, "Multi-mode wave propagation in ribbed plates : Part i k-space characteristics," *International Journal of Solids and Structures* **45**(5), pp. 1179–1195, 2008.

[21] G. Floquet, "Sur les quations diffrentielles linaires coefficients priodiques," *Annales de l'Ecole Normale Suprieure* **12**, pp. 47–88, 1883.

[22] F. Bloch, "ber die Quantenmechanik der Electron in Kristallgittern," *Zeitschrift fr Physik* **52**, pp. 550–600, 1928.

[23] M. Collet, M. Ouisse, M. Ichchou, and M. Ruzzene, "Numerical tools for semi-active optimization of 2d waves dispersion into mechanical system," in *ASME-SMASIS*, ASME, (Philadelphia), Sept 28 Oct 1 2010.

[24] J. Joannopoulos, R. Meade, and J. Winn, *Photonic Crystals: Molding the Flow of Light*, Princeton University Press, 1995.

[25] C. Kittel, *Introduction to Solid State Physics*, John Wiley and Sons, New York, 1986.

[26] A. Bensoussan, J. Lions, and G. Pananicolaou, *Asymptotic Analysis for Periodic Structures*, North Holland, 1978.

[27] G. Allaire and C. Congas, "Bloch waves homogenization and spectral asymptotic analysis," *Journal de Mathmatiques Pures et Appliques* **77**, pp. 153–208, 1998.

[28] M. N. Ichchou, S. Akrout, and J. Mencik, "Guided waves group and energy velocities via finite elements," *Journal of Sound and Vibration* **305**, pp. 931–944, SEP 11 2007.

[29] L. Houillon, M. Ichchou, and L. Jezequel, "Wave motion in thin-walled structures," *Journal of Sound and Vibration* **281**, pp. 483–507, MAR 22 2005.

[30] J. Mencik and M. Ichchou, "Multi-mode propagation and diffusion in structures through finite elements," *European Journal of Mechanics A-Solids* **24**, pp. 877–898, SEP-OCT 2005.

[31] W. Maysenhölder, *Körperschall-energie Grundlagen zur Berechnung von Energiedichten und Intensitäten*, Wissenschaftliche Verlagsgesellschaft, Stuttgart, 1994.

[32] N. W. Hagood and A. H. von Flotow, "Damping of structural vibrations with piezoelectric materials and passive electrical networks," *Journal of Sound and Vibration* **146(2)**, pp. 243–268, 1991.

[33] M. Collet and K. Cunefare, "Modal Synthesis and Dynamical Condensation Methods for Accurate Piezoelectric Systems Impedance Computation," *Journal of Int Mat Syst and Struct* **19**(11), pp. 1251–1271, 2008.

[34] F. Casadei, M. Ruzzene, B. Beck, and K. Cunefare, "Vibration control of plates featuring periodic arrays of hybrid shunted piezoelectric patches," in *Proceedings of SPIE - Smart Structures and Materials*, **7288**, SPIE, 2009.

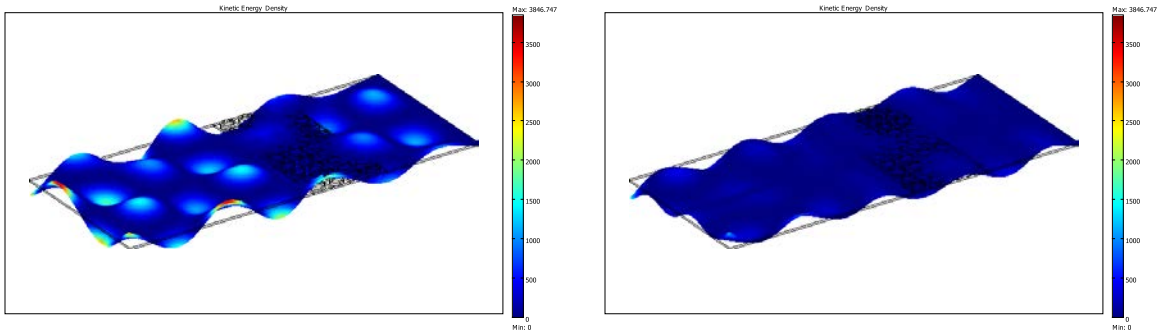

(a) 5 kHz

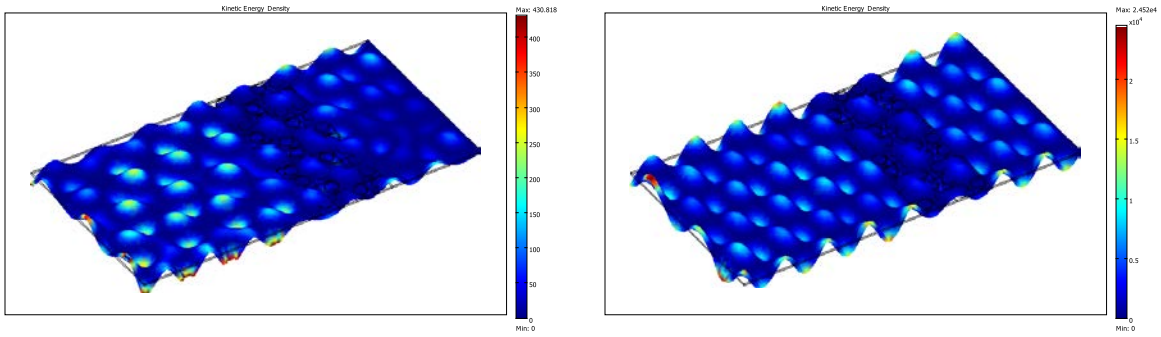

(b) 22 kHz

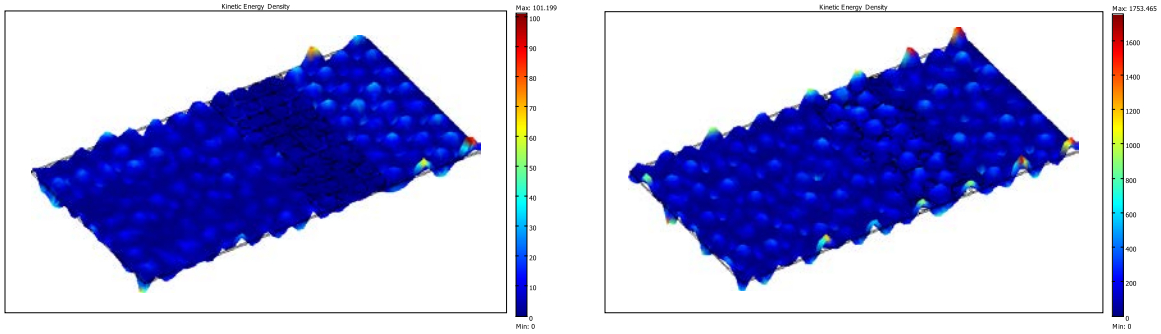

(c) 60 kHz

Figure 9. Kinetic Energy density for different source frequency ((a) 5 kHz, (b) 22 kHz, (c) 60 kHz). On the left with optimal impedance connected to the piezo-patches and on the right with open circuit